Proc. NIPR Symp. Polar Meteorol. Glaciol., **11**, 117-126, 1997

LIDAR OBSERVATIONS ABOVE NY-ÅLESUND, SVALBARD, NORWAY DURING WINTER 1995/96

Kouichi SHIRAISHI[1], Motowo FUJIWARA[1], Yasunobu IWASAKA[2], Takashi SHIBATA[2], Masahiro NAGATANI[2], Hiroshi ADACHI[2], Tetsu SAKAI[2] and Kazuhiro FUJINO[1]

[1]*Department of Applied Physics, Fukuoka University, Jonan-ku, Fukuoka 814-80*
[2]*Solar Terrestrial Environment Laboratory, Nagoya University, Chikusa-ku, Nagoya 464-01*

Abstract: Lidar observations of stratospheric aerosols were performed in the winter of 1995/96 at Ny-Ålesund, Svalbard in Norway (79°N, 12°E). Superposed on the usual aerosol layer, polar stratospheric clouds (PSCs) were observed intermittently between December 1995 and February 1996. The temperature at the heights of the PSCs was very low, below the estimated frost point of nitric acid trihydrate (NAT). PSC observed initially at the appearance of cold air always consisted of solid particles. Each height distribution of scattering ratio (R) and depolarization (δ) ratio has a single peak, and the relation between R and δ shows a positive correlation at the edge of the horizontal extent of the PSC layer. As the cold area developed, PSC layers with negative correlation between R and δ were frequently detected, as they had been in previous observations.

1. Introduction

The polar stratosphere has received increased attention since the detection of the Antarctic springtime ozone depletion phenomenon by FARMAN *et al.* (1985). Although no large ozone losses in the Arctic region have been observed, polar stratospheric clouds (PSCs) are expected to be of importance for the ozone chemistry within the cold polar stratosphere. Especially, PSC type I clouds have been observed frequently in the Arctic region in past years. DC-8 lidar observations during the AASE in the Arctic show that PSC-I clouds are classified into two subclasses of Type I PSC clouds, Type Ia and Ib, based on the scattering and depolarization behavior of the cloud particles (BROWELL *et al.*, 1990). It is generally believed that Type Ia particles are large and nonspherical (radius$>1\ \mu$m), while Type Ib particles are small and spherical based on theoretical analysis (TOON *et al.*, 1990). Recently, however, various types of PSC have been observed which could not be classified into either, type Ia or Ib (SHIBATA *et al.*, 1996).

We set a lidar station at Ny-Ålesund, Svalbard, Norway in September 1993 and have performed observations in every winter since January 1994.

In this paper we focus on the results of PSC observations in the 1995/96 winter. First we discuss the features and temporal behavior of detected PSC, and second the temperature dependence of PSCs which were observed.

2. Measurements

Observations were made using an Nd : YAG lidar at both the fundamental (1064 nm) and second harmonic (532 nm) wavelengths. The output energy of the laser is about 150 mJ/pulse at each wavelength with the pulse repetition rate of 10 Hz. Backscattered light was collected by a 35 cm Schmidt Cassegrainian telescope and split into four channels of the light detecting system, each including a photomultiplier, an interference filter and some other optics. Two channels detected signals in planes parallel and perpendicular to the primary polarization plane of the transmitted laser light (532 nm). The other two channels measured the fundamental signal and the Raman scattering signal from N_2 molecules.

The physical properties of particulates are described in terms of the scattering ratio R at 532 nm , the depolarization ratio δ at 532 nm, and the Angstrom coefficient α.

R is defined as $R=(\beta_R+\beta_M)/\beta_R$, where β_R and β_M are the molecular and aerosol backscattering coefficients respectively, and is roughly proportional to the mass mixing ratio of particulate matter. δ is defined as $\delta=\beta_\perp/(\beta_\perp+\beta_{||})$, where $\beta_\perp$ and $\beta_{||}$ are the backscattering coefficients for the perpendicular and parallel returns, respectively. δ is zero if the particles are spherical particulates such as liquid droplets. For nonspherical particles such as crystallized aerosols, δ is high. The Angstrom coefficient α shows the wavelength dependence of the aerosol backscattering. It is assumed to be proportional to $\lambda^{-\alpha}$, where λ is the laser wavelength. It is defined as $\alpha=4-\ln(R(1064)/R(532))/\ln(1064/532)$, where $R(1064)$ and $R(532)$ are the scattering ratios at 1064 nm and 532 nm, respectively. Since the molecular backscattering is proportional to λ^{-4}, α represents the contribution of the particulates. If the value of α is larger, the size distribution is considered to be shifted toward smaller sizes.

3. Lidar Observation

Lidar observations were carried out from November 1995 to February 1996. Figure 1 shows the temporal development of temperature in the upper troposphere and lower stratosphere during the observation period over Ny-Ålesund. Original data were supplied by courtesy of AWI. Roughly speaking, the cold region below 193 K appeared three times (12/1-12/2, 12/17-1/30, 2/3-2/24) during the observation period, when PSCs were often detected.

The first cold area appeared in the vicinity of height 22 km in early December 1995, then the first PSC was detected at the same height. Figure 2 shows the profiles of R, δ and α observed on December 1, 1995. The peaks of both R and δ can be seen between 21 and 25 km in the cold area where temperature is lower than the frost point of NAT, which is estimated using the vapor equilibrium equation (HANSON and MAUERSBERGER, 1988) under the assumption that the air mass of interest has mixing ratios of 5 ppmv H_2O and 10 ppbv HNO_3, respectively. The values of α in this range is about 1, which is lower than the values (1.4～2.5) of α for background aerosols in the range of 12-20 km. This shows that PSC particles are larger than the background aerosols. The peak values of R and δ are 1.3 and 0.02, respectively, at the same height, about 22 km. The peak height of R coincides with that of δ, which shows the positive correlation between R and δ. PSCs observed in December 1995 showed positive correlation frequently, while most PSCs

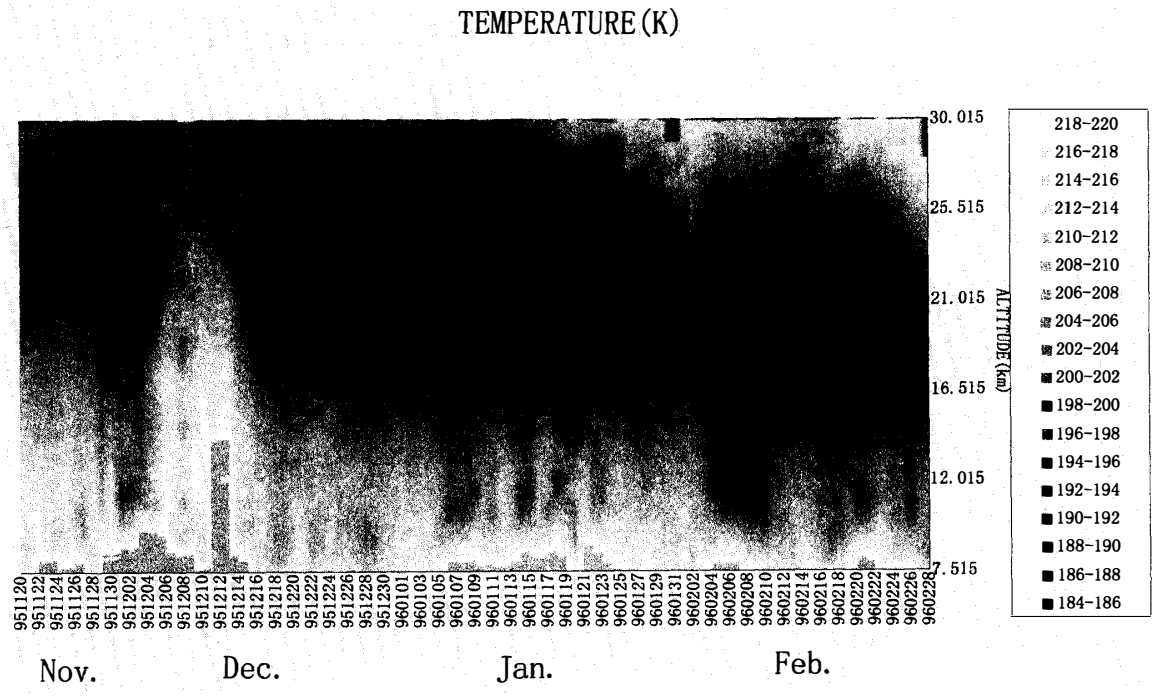

Fig. 1. The temporal development of temperature in the upper troposphere and lower stratosphere over Ny-Ålesund, Norway.

observed in winter 1994/95 showed negative correlation between R and δ. We could not observe on December 2-3 because of bad weather. On December 7 PSC disappeared consistently with the increase of stratospheric temperature.

The cold area ($T<193$ K) appeared again on December 17, 1995, and PSCs were detected as shown in the positive correlation between R and δ, too. As a cold area developed, both R and δ of the PSC layer detected were becoming very variable quantitatively, R reached a maximum on December 23. Figures 3 and 4 show typical profiles observed in this period, on December 22. The PSC layer at 0452-0804 (UT) exists in the region from 19 to 25 km where the temperature was 2-6 K lower than the NAT frost point. Here R and δ height distributions show positive correlation. Corresponding to the peaks of both R and δ, α is a minimum. The profile at 0947-1220 after about 3 hours is quite different. R has two peaks, at 20.5 and 24 km, which sandwich the small peak of δ at 22.5 km. It is composed of 4 different type sublayers (20-21, 21-22, 22-23.8, 23.8-25 km), a "sandwich structure" as pointed out by SHIBATA (SHIBATA *et al.*, 1996). It seems that α took large values (>1) in the region of enhanced R and a minimum value at the height of the R minimum rather than the δ maximum. As shown in Figs. 3 and 4, the optical structure of PSCs observed varied drastically in only about 3 hours. The time scale of such variation is about 2 to 6 hours.

During the period of 26-28 December 1995, only small echoes by PSCs ($R<1.2$, $0.5<\delta<0.01$) were detected, possibly due to the lack of materials such as nitric acid vapor and water vapor in the air mass above the station.

Figure 5 shows a typical profile observed in early January 1996. The cold area grew rapidly in the period to the fully developed stage in mid-January 1996. R shows large and

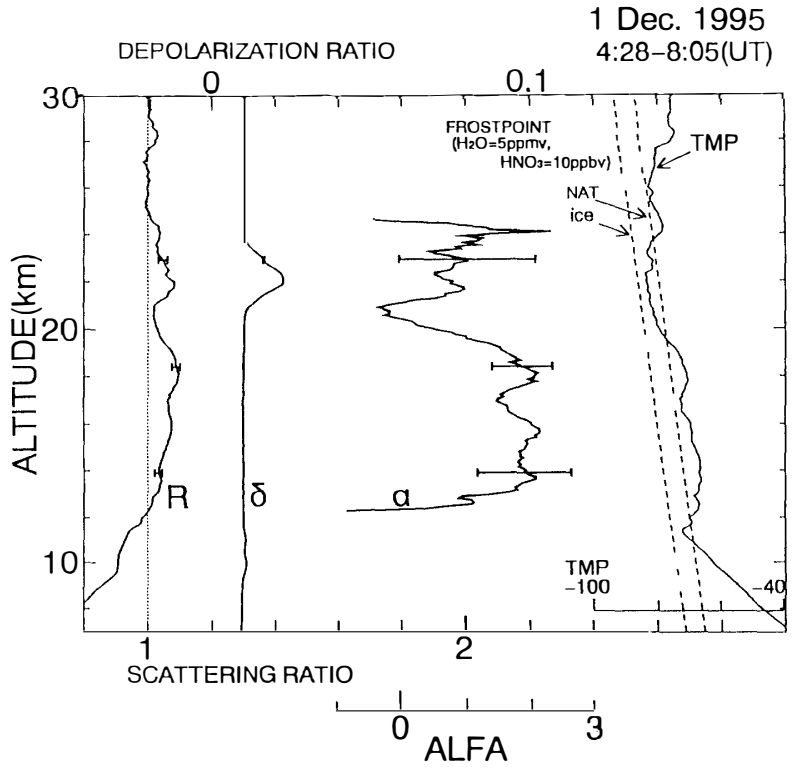

Fig. 2. Vertical profile of backscattering ratio (532 nm), depolarization ratio (532), Angstrom coefficient, temperature and estimated NAT frost point observed from 0428 to 0805 on 1 December 1995.

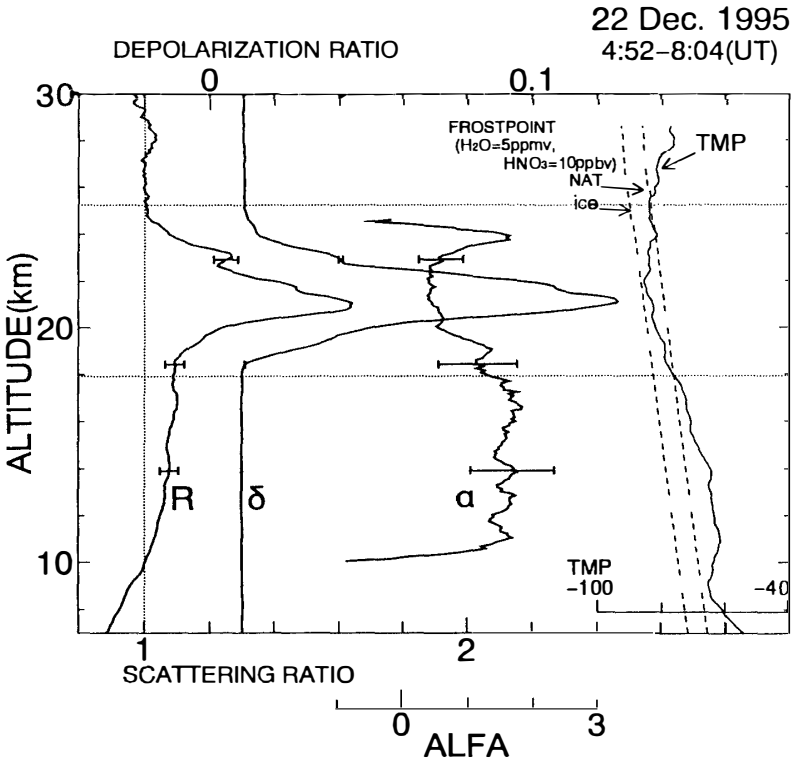

Fig. 3. Same as Fig. 2 but for from 0452 to 0804 on 22 December 1995.

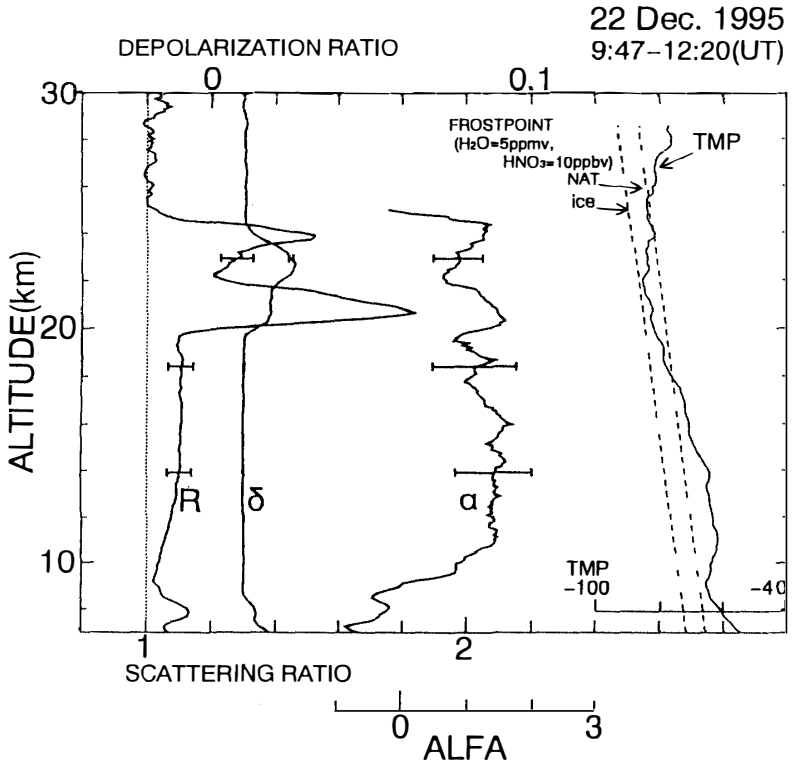

Fig. 4. Same as Fig. 2 but for from 0947 to 1220 on 22 December 1995.

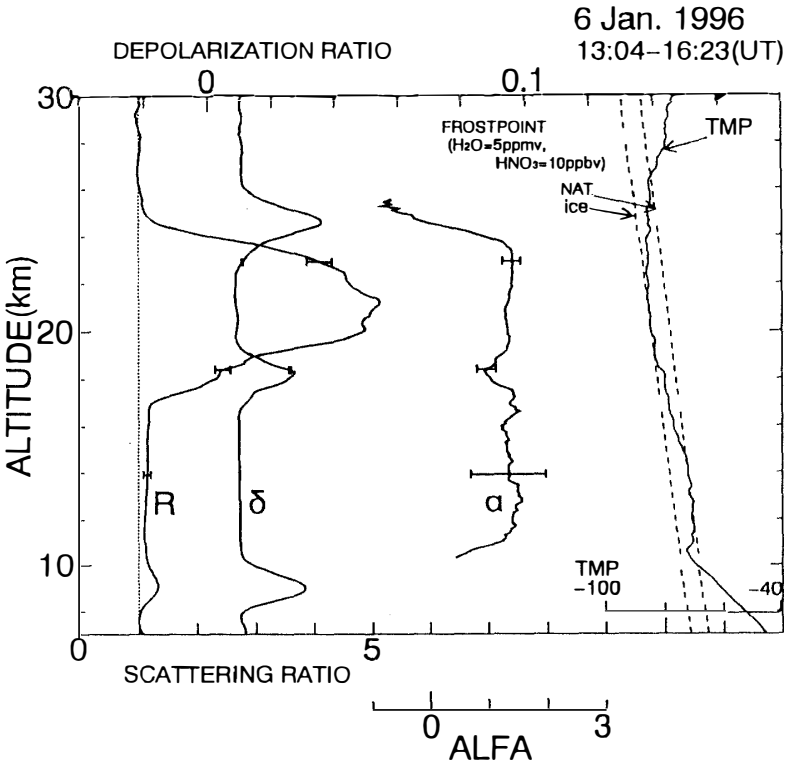

Fig. 5. Same as Fig. 2 but for from 1304 to 1623 on 6 January 1996.

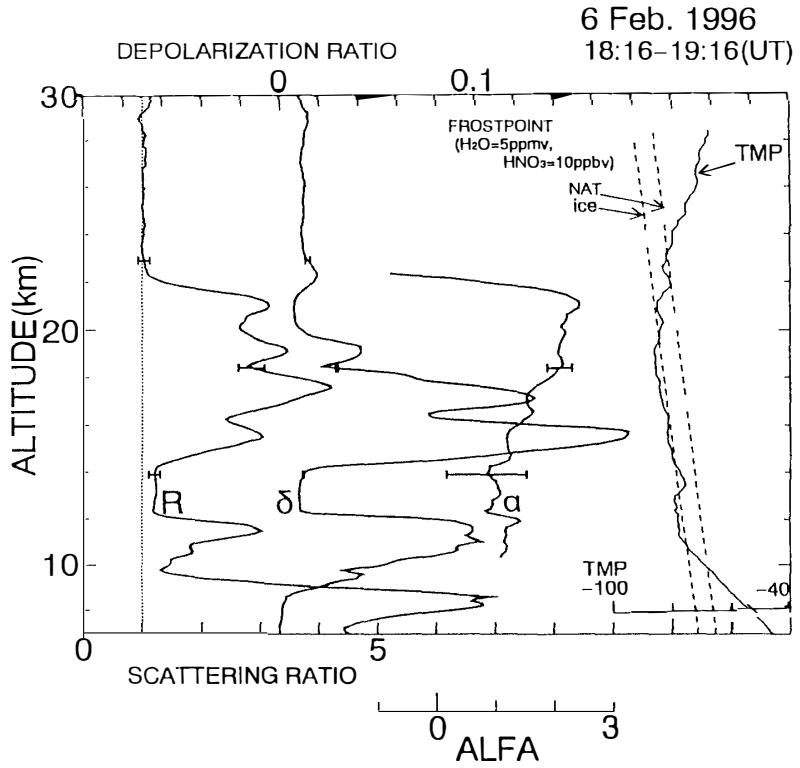

Fig. 6. Same as Fig. 2 but for from 1816 to 1916 on 6 February 1996.

broad enhancement in the height range 17–26 km. The peaks of δ were observed at both the top and bottom of the layer. α took a minimum at the lower peak height of δ (18 km). PSCs observed on January 6, 1996 were also composed of multiple layers. The height distributions of R, δ and α were complicated, such as those observed on December 22. During a few days after January 5, 1996 when the lower stratospheric temperature was lower than the water ice frost point, PSCs of the sandwich structure mentioned above were frequently observed. Such PSC layers were observed in winter 1994/95 at a fully developed stage of the cold stratosphere. The time variation of the PSC observed on January 6, 1996 is not remarkable.

In early February 1996, the cold area appeared in a height range lower than the previous cold area. On February 6, 1996 (Fig. 6), the temperature was lower than the NAT frost point in the height range of 10–23.5 km, and large and broad enhancement in both R and δ were observed. The physical properties of PSCs in the region above 20 km are quite different from those in the lower region. The correlation between R and δ is negative in the upper region and positive in the lower region. Considering the tropopause height, it is possible to identify the lower clouds at 10–12 km as PSCs.

4. The Pattern of Appearance and Behavior of PSC

Figure 7a shows the hourly averaged profiles of scattering ratio, and 7b the depolarization rate observed on December 1, 1995. The PSC layer was observed in the height range 20–24 km. The enhancement of δ was detected from 0428 to 1048, followed by increase

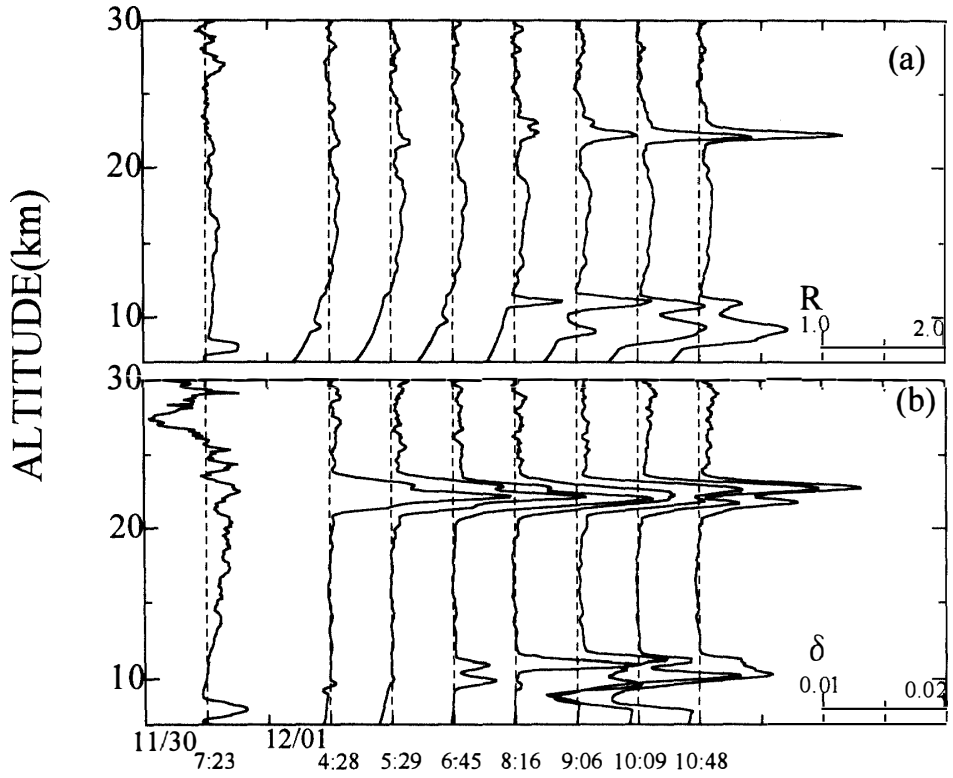

Fig. 7. Hourly averaged profiles of scattering ratio (a) and depolarization rate (b) observed on 1 December 1995.

of R from 0816 at the same altitude. There are two possible interpretations for this process. One is that nonspherical particles such as crystallized aerosols were produced at first and then increased rapidly. The other is that the edge of the horizontal extent of the detected PSC layer had such distribution in R and δ. Nonspherical particles were early detected at the beginning of the appearance of PSCs, although recent laboratory experiments suggest that it is difficult to produce crystallized particles prior to liquid particles, especially above the ice frost point (KOOP *et al.*, 1995; HAMILL *et al.*, 1996). Such a pattern of PSC was observed not only in early December 1995 but also mid-December, 1995 and early January 1996.

Figure 8 shows the temporal behavior of the correlation coefficient between R and δ in the height range where PSC layers were detected. We define the height range of PSCs as the range where R and δ show significant enhancement, as shown in Fig. 3 by two dotted lines. In early and mid December 1995 just after the appearance of the cold area above Ny-Ålesund, correlation coefficients vary from 0.6 to 1. Each height profile of R and δ shows a single peak roughly at the same height as seen in Fig. 2. As the cold area developed, a PSC layer with negative correlation between R and δ appeared frequently. Such a trend can also be seen in early February 1996. Considering the motion of the air mass above Ny-Ålesund, the data in Fig. 8 might show that the horizontal edge of the PSC layer has positive correlation between R and δ and includes more crystallized particles than liquid particles. As the temperature decreased to near the ice frost point (5 ppmv), we frequently detected PSCs with negative correlation between R and δ. Positive correlation

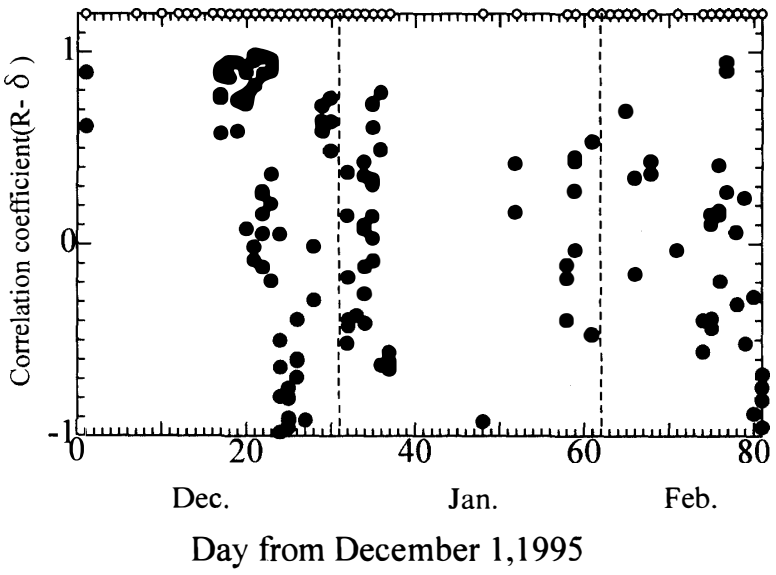

Fig. 8. Temporal behavior of the correlation between backscattering ratio (532) and depolarization rate in the PSC height range. The circles above the plot indicate times of lidar operation.

shows that the increase of backscattering from PSCs is caused by the formation of frozen particulates. Negative correlation is a little difficult to interpret but may show that the main part of the PSC layer is formed by the supercooled liquid droplets although the upper and/or lower side of the layer remain frozen. The observed PSCs are the mixing of these types as shown in Figs. 4 and 5. Generally speaking, the layers of positive correlation appeared in the colder region but sometimes both types appeared at almost the same temperature. Some recent theories suggest that each of the layers has a different mechanism of formation which is associated with its own temperature history.

5. The Temperature Dependence on Scattering Ratio and Depolarization Ratio of PSCs

Figures 9 and 10 show the correlation between the scattering ratio and temperature difference dT ($dT = T$-estimated frost point of NAT), and between the depolarization ratio and dT, respectively, at the height range of 18–22 km where PSCs were frequently observed. They also include background aerosol data. The region where the dots are concentrated in those figures shows the contribution by the background sulphate aerosol layer. The enhancement of the depolarization ratio appeared at temperature 2–3 K lower than the estimated frost point of NAT. The increase of scattering ratio appeared when the temperature was 2–3 K lower than that of enhancement of δ. As mentioned in Section 4, at the first appearance of PSC, the enhancement of δ was detected first, followed by the increase of R. Enhancement of δ was detected at temperature 1–2 K higher than the estimated frost point of NAT. This might be due to the underestimate of the assumed vapor pressure of nitric acid or water, or the hysteresis effect of aerosol particles. If the latter is the correct explanation, it would have an important effect on the denitrification

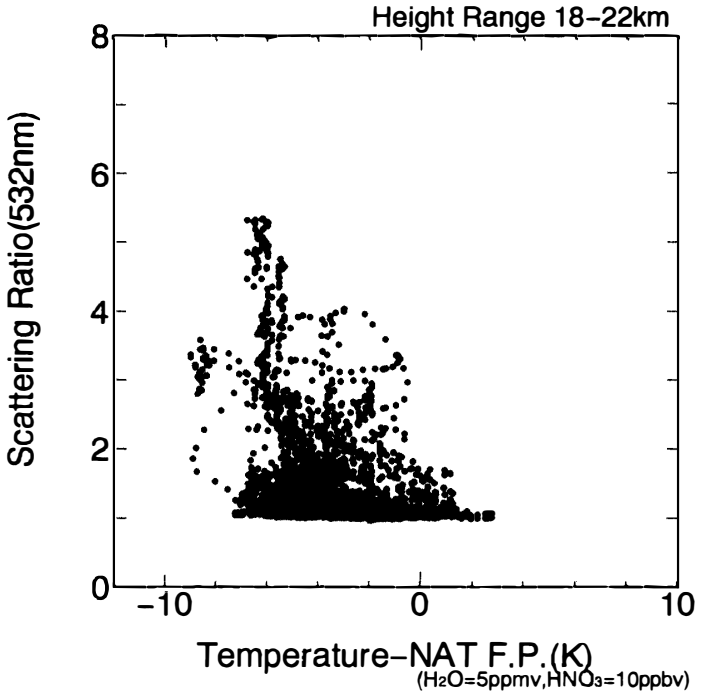

Fig. 9. The correlation of all PSC profile scattering ratios and temperature differences dT (dT = T-estimated frost point of NAT) in the height range 18–22 km.

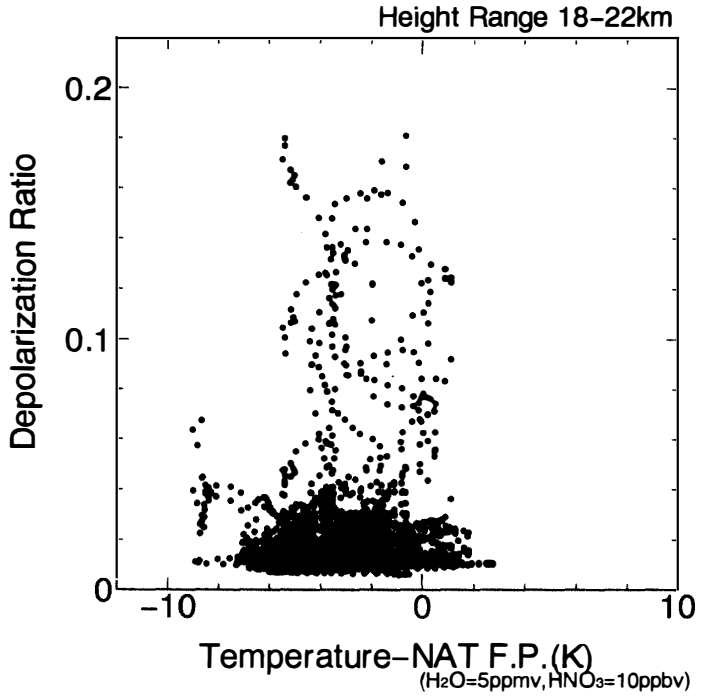

Fig. 10. The correlation of all PSC profile depolarization ratios and temperature differences dT (dT = T-estimated frost point of NAT) in the height range 18–22 km.

process in the stratosphere.

6. Conclusion

Lidar observations were performed from 20 November 1995 to 28 February 1996 at Ny-Ålesund in Norway. PSCs were frequently observed in the cold area where the temperature was lower than the NAT frost point. At the beginning of stratospheric cooling, PSCs with non-spherical particles were observed. R and δ have single peaks and show positive correlation with each other. As the cooling developed, PSCs with negative correlation were observed. The time scale of the variation was about 2 to 6 hours. As the temperature decreased, close to the ice frost point (5 ppmv), PSCs of optical multi-layer structure were frequently observed.

In view of the temperature dependence of the scattering ratio and depolarization ratio of PSCs, enhancement of the depolarization ratio appeared at 0–2 K lower than the estimated NAT frost point, while the increase of the scattering ratio was 2–3 K lower than that. We also detected non-spherical particles at a temperature 1–2 K higher than that of the estimated frost point of NAT. This might be due to the histeresis effect of aerosol particles.

Acknowledgments

The radiosonde data used here were kindly provided by the Alfred Wegener Institute which has always been of great support. We also wish to thank Kings Bay Kull Company (KBKC).

References

BROWELL, E.V., BUTLER, C.F., ISMAIL, S., ROBINETTE, P.A., CARTER, A.F., HIGDON, N.S., TOON, O.B., SCHOEBERL, M.R. and TUCK, A.F. (1990): Airbone lidar observations in the wintertime Arctic stratosphere: Polar stratospheric clouds. Geophys. Res. Lett., **17**, 385–388.

FARMAN, J.C., GARDINER, B.C. and SHANKLIN, J.D. (1985): Large losses of total ozone in Antarctica reveal seasonal ClO_x/NO_x interaction. Nature, **315**, 207–210.

KOOP, T., BIERMANN, U.M., RABER, W., LUO, B.P., CRUTZEN, P.J. and PETER, Th. (1995): Do stratospheric aerosol droplets freeze above the ice frost point? Geophys. Res. Lett., **22**, 917–920.

HAMILL, P., TABAZADEH, A., KINNE, S., TOON, O.B. and TURCO, R.P. (1996): On the grouth of ternary system $HNO_3/H_2SO_4/H_2O$ aerosol particles in the stratosphere. Geophys. Res. Lett., **23**, 753–756.

HANSON, D. and MAUERSBERGER, K. (1988): Laboratory studies of nitric acid trithydrate: implications the south polar stratosphere. Implications for the south polar stratosphere. Geophys. Res. Lett., **15**, 855–858.

SHIBATA, T., IWASAKA, Y., FUJIWARA, M., HAYASHI, M., NAGATANI, M., SHIRAISHI, K., ADACHI, H., SAKAI, T., SUSUMU, K. and NAKURA, Y. (1996): Polar stratospheric clouds observed by a lidar over Spitsbergen in the winter 1994/1995: Liquid particle and vertical "Sandwich" structure. J. Geophys. Res., **102**, 10829–10840.

TOON, O.B., BROWELL, E.V., KINNE, S. and JORDAN, J. (1990): An analysis of lidar observations of polar stratospheric clouds. Geophys. Res. Lett., **17**, 393–396.

(Received December 25, 1996; Revised manuscript accepted June 19, 1997)